of $CuBr(PPh_3)_3$, $(6.45 \pm 0.04) \times 10^3$ M^{-1} cm^{-1}.[19]

Quantum-yield data provide the second source of information about the nature of the sensitizer formed upon $CuBr(py)(PPh_3)$. of a several-fold excess of PPh_3 to solutions of $CBr(py)(PPh_3)$. If we again assume that all of the $CuBr(py)(PPh_3)$ originally present is converted to $CuBr(PPh_3)_3$, eq 11 can be used to calculate the intrinsic quantum yield of sensitization (last column in Table I). Both the reasonable constancy of ϕ_{in} (0.33 ± 0.03) at PPh_3:Cu ratios ≥ 10 and the close agreement with the ϕ_{in} values determined for $CuBr(PPh_3)_3$ itself (Table II) substantiate the assignment of this Cu(I) species as the key sensitizer in the system.

(c) Summary Comments. The present study establishes that the mechanism by which Cu(I) sensitizes an olefin photoreaction can be dictated by the addition of suitable ligands to the system. This effect has its origin in the facile[21] ligand addition and/or substitution processes that convert the original copper(I) compound into one or more new species. Thus the addition of NBD to a solution containing $CuBr(py)(PPh_3)$ results in the formation of a ground-state Cu(I)–NBD complex that, upon the absorption of a photon, generates a molecule of Q. This sensitization pathway can be blocked by ligands such as py and PPh_3 that effectively compete with NBD for a coordination site about copper. In the presence of sufficient PPh_3 to form $CuBr(PPh_3)_3$, the predominant mechanism of sensitization changes to one involving bimolecular interaction of the photoexcited Cu(I) compound and ground-state NBD.

The effectiveness of $CuBr(PPh_3)_3$ as a sensitizer stands in sharp contrast to the behavior of $CuBr(py)_2PPh_3$ (eq 6) and $CuBr(py)(PPh_3)_2$ (presumed to be formed upon addition of less than an equimolar amount of PPh_3 to $CuBr(py)(PPh_3)$). It is possible that this disparity reflects differences in orbital parentage of the lowest electronic excited state. This state in $CuBr(PPh_3)_3$ appears to be largely localized on PPh_3, while the py-containing compounds possess low-lying Cu → py charge-transfer states (see Figure 4 and accompanying discussion). Whether the inability of this latter excited state to sensitize the NBD to Q rearrangement reflects its lower energy or an exceedingly rapid deactivation to the ground state remains an interesting question deserving further study.

Acknowledgment. We thank the U.S. Department of Energy for support of this work under Contract EY-76-S-09-0893 and Grant DE-FG02-79ER-10540.

Registry No. $CuBr(py)(PPh_3)$, 25753-77-9; $CuBr(PPh_3)_3$, 15709-74-7; NBD, 121-46-0; PPh_3, 603-35-0; py, 110-86-1; Q, 278-06-8.

(21) Rapid exchange between the first coordination sphere of Cu(I) and bulk solution has been reported for uncharged ligands such as phosphines and olefins: Muetterties, E. L.; Alegranti, C. W. *J. Am. Chem. Soc.* **1970**, *92*, 4114. Salomon, R. G.; Kochi, J. K. *Ibid.* **1973**, *95*, 1889.

Contribution from the Departments of Chemistry, The University of Texas at Austin, Austin, Texas 78712, Southern Methodist University, Dallas, Texas 75275, and Iowa State University, Ames, Iowa 50010

UV Photoelectron Spectroscopic Investigation of Some Polycyclic Group 5A Compounds and Related Acyclic Species. 1. Free and Coordinated Aminophosphines and Related Compounds

A. H. COWLEY,*[1a] M. LATTMAN,*[1b] P. M. STRICKLEN,[1c] and J. G. VERKADE*[1c]

Received March 25, 1981

He I ultraviolet photoelectron (UV PES) spectra are reported for $XP(NMeCH_2)_3CMe$ (X = O (**1A**), S (**1B**), Se (**1C**), BH_3 (**1D**)), the rigid tricyclic $XP(NCH_2CH_2)_3$ (X = O (**2A**), S (**2B**), Se (**2C**)), the adamantane-like molecules urotropine (**3**) and $XP(CH_2N)_3(CH_2)_3$ (X = lone pair (**5**), O (**5A**), S (**5B**), Se (**5C**)), $XP(CH_2N)(CH_2)_2(CH_2CH_2)$ (X = lone pair (**6**), O (**6A**)), and $XP(NMe_2)_3$ (X = O (**7A**), S (**7B**), Se (**7C**), BH_3 (**7D**)). The present spectral data are compared to those previously recorded for $P(NMeCH_2)_3CMe$ (**1**), $MeC(CH_2NCH_2)_3$ (**4**), and $P(NMe_2)_3$ (**7**).

Introduction

Ultraviolet photoelectron spectroscopy (UV PES) has been shown to be a useful tool for studying molecular conformation and bonding in the gas phase.[2] The utility of the UV PES experiment in these respects stems largely from the patterns that are associated with the ionizations from orbitals possessing appreciable lone-pair character.[3] Interpretational difficulties can arise with this approach, however, particularly when several conformations are possible and/or the lone-pair orbitals of the various heteroatoms are close in energy. A case in point concerns the acyclic aminophosphines,[2a,d,f,h] where doubts persist not only about the UV PES assignments but also about the ground-state structures. The present work was carried out in an attempt to resolve these residual uncertainties (a) by broadening the scope of our previous UV PES work[2f] on rigid, polycyclic PN_3 systems possessing either well-established structures or geometries that can be confidently inferred and (b) by examining the spectral changes that ensue upon coordination of the phosphorus lone pair to various Lewis acids. A subsequent paper will be concerned with similar studies of phosphite, arsenite, and thiophosphite esters.

Results and Discussion

The UV PES data for the compounds studied are summarized in Table I. The data and assignments pertain primarily to lone-pair ionizations; however, other ionizations have been

(1) (a) The University of Texas at Austin. (b) Southern Methodist University. (c) Iowa State University.

(2) See, for example: (a) Cowley, A. H.; Dewar, M. J. S.; Goodman, D. W.; Schweiger, J. R. *J. Am. Chem. Soc.* **1973**, *95*, 6506. (b) Cowley, A. H.; Dewar, M. J. S.; Goodman, D. W.; Padolina, M. C. *Ibid.* **1974**, *96*, 2648. (c) Ames, D. L.; Turner, D. W. *J. Chem. Soc., Chem. Commun.* **1975**, 179. (d) Lappert, M. F.; Pedley, J. B.; Wilkins, B. T.; Stelzer, O.; Unger, E. *J. Chem. Soc., Dalton Trans.* **1975**, 1207. (e) Cowley, A. H. *Phosphorus Sulfur* **1976**, *2*, 282. (f) Cowley, A. H.; Goodman, D. W.; Kuebler, N. A.; Sanchez, M.; Verkade, J. G. *Inorg. Chem.* **1977**, *16*, 854. (g) Cowley, A. H.; Lattman, M.; Montag, R. A.; Verkade, J. G. *Inorg. Chim. Acta* **1977**, *25*, L151. (h) Hargis, J. H.; Worley, S. D. *Inorg. Chem.* **1977**, *16*, 1686. (i) Cowley, A. H.; Dewar, M. J. S.; Lattman, M.; Mills, J. L.; McKee, M. *J. Am. Chem. Soc.* **1978**, *100*, 3349. (j) Yarbrough, L. W.; Hall, M. B. *Inorg. Chem.* **1978**, *17*, 2269. (k) Cowley, A. H.; Lattman, M.; Walker, M. *J. Am. Chem. Soc.* **1979**, *101*, 4074. (l) Chisholm, M. H.; Cowley, A. H.; Lattman, M. *Ibid.* **1980**, *102*, 46.

(3) For a review, see: Hoffman, R. *Acc. Chem. Res.* **1971**, *4*, 1.

0020-1669/82/1321-0543$01.25/0

Table I. Ionization Energies and Interaction Parameters[a] for Free and Coordinated Aminophosphines and Related Compounds

compd	X	no.	IE_N	$\overline{IE}_N$	IE_P	IE_X	interaction parameters, β_{NN}
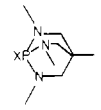	lp[m]	1	7.71 (a_2)[b] 8.59 8.76 } (e)[d]	8.35	9.03 sh (a_1)[c]		0.32
	O	1A	8.14 (a_2) 8.99 9.24 } (e)[d]	8.79		10.4 (e)	0.33
	S	1B	8.14 (a_2) 9.14 9.31 } (e)[d]	8.86		8.62 (e)	0.36
	Se	1C	8.15 (a_2)[e] 9.02 9.23 } (e)[d]	(8.8)[f]		8.15 (e)[e]	(0.33)
	BH_3	1D	8.13 (a_2) 9.04 9.23 } (e)[d]	8.80		10.0 (e)[g]	0.34
	O	2A	8.89 (e) 10.21 10.44 sh } (a)[e]			10.21 10.44 sh } (e)[e]	
	S	2B	8.43 (e) 9.97 (a_1)	8.94	11.8 (a_1)[h]	9.10 (e)	0.53
	Se	2C	8.32 8.8 sh } (e)[e] 10.02 (a_1)			8.32 8.8 } (e)[e]	
		3	8.55 (t_2) 12.2 (a_1)[i]				0.91[i]
		4[j]	8.08 (e) 9.90 (a_1)	8.69			0.61
	lp	5	8.05 (e)[e] 11.8 (a_1)[k,l]		8.3 sh (a_1)[e,k]		
	O	5A	8.19 (e) 10.66 (a_1)[e]	(9.0)	11.7 (a_1)[h]	10.66 (e)[e]	0.82
	S	5B	8.02 (e) 10.32 (a_1)	8.79		9.24 (e)	0.77
	Se	5C	7.89 (e) 10.18 (a_1)	8.65	11.6 (a_1)[h]	8.94 (e)	0.76
	lp	6	7.35 (a'') 8.22 (a')[e] 10.30 (a')[k]		8.22 (a')[e,k]		
	O	6A	7.63 (a'') 8.40 (a') 9.59 (a')	8.54		10.5	
$XP[N(CH_3)_2]_3$	lp	7	7.89 (a'') 8.77 (a') 9.90 (a')[k]		7.58 (a')[k]		
	O	7A	8.27 (a'') 8.72 (a') 9.13 (a')	8.71		10.47 (a', a'')	0.23
	S	7B	8.63 (a'') 9.09 (a') 9.57 (a')	9.10	12.0 (a')[h]	8.04 (a', a'')	0.23
	Se	7C	8.45 (a'') 8.98 (a') 9.41 (a')	8.95	11.7 (a')[h]	7.75 (a', a'')	0.27
	BH_3	7D	8.31 (a'') 8.55 (a') 9.30 (a')	8.72		9.9 (a', a'')[g]	0.12

[a] In eV. [b] Orbital symmetry assignments in parentheses. [c] Shoulder. [d] Jahn-Teller split ionization band. [e] Overlapping bands. [f] Values in parentheses are uncertain (±0.1 eV) due to overlapping bands. [g] First maximum of a very broad IE band due to BH_3 group. [h] σ_{PX} ionization. [i] These values are lower limits. [j] Data from ref 21a. [k] Interacting n_N/n_P orbitals; see text. [l] Lower limit, see text. [m] lp = lone pair.

assigned when feasible. For convenience, formulas (structures when relevant) for the compounds are presented in Table I along with pertinent reference numbers in the text. The compound numbering system is such that the free (uncomplexed) base is given only a number while the various complexes are given a number and letter. Each letter represents a specific complex, thus **A** = oxygen, **B** = sulfur, **C** = selenium, and **D** = borane.

Polycyclic Systems. Definitive structural data are not available for **1**. However, the X-ray crystal structures of the corresponding phosphine oxide, **1A**, and the borane complex, **1D**, have been determined.[4] In the present context the im-

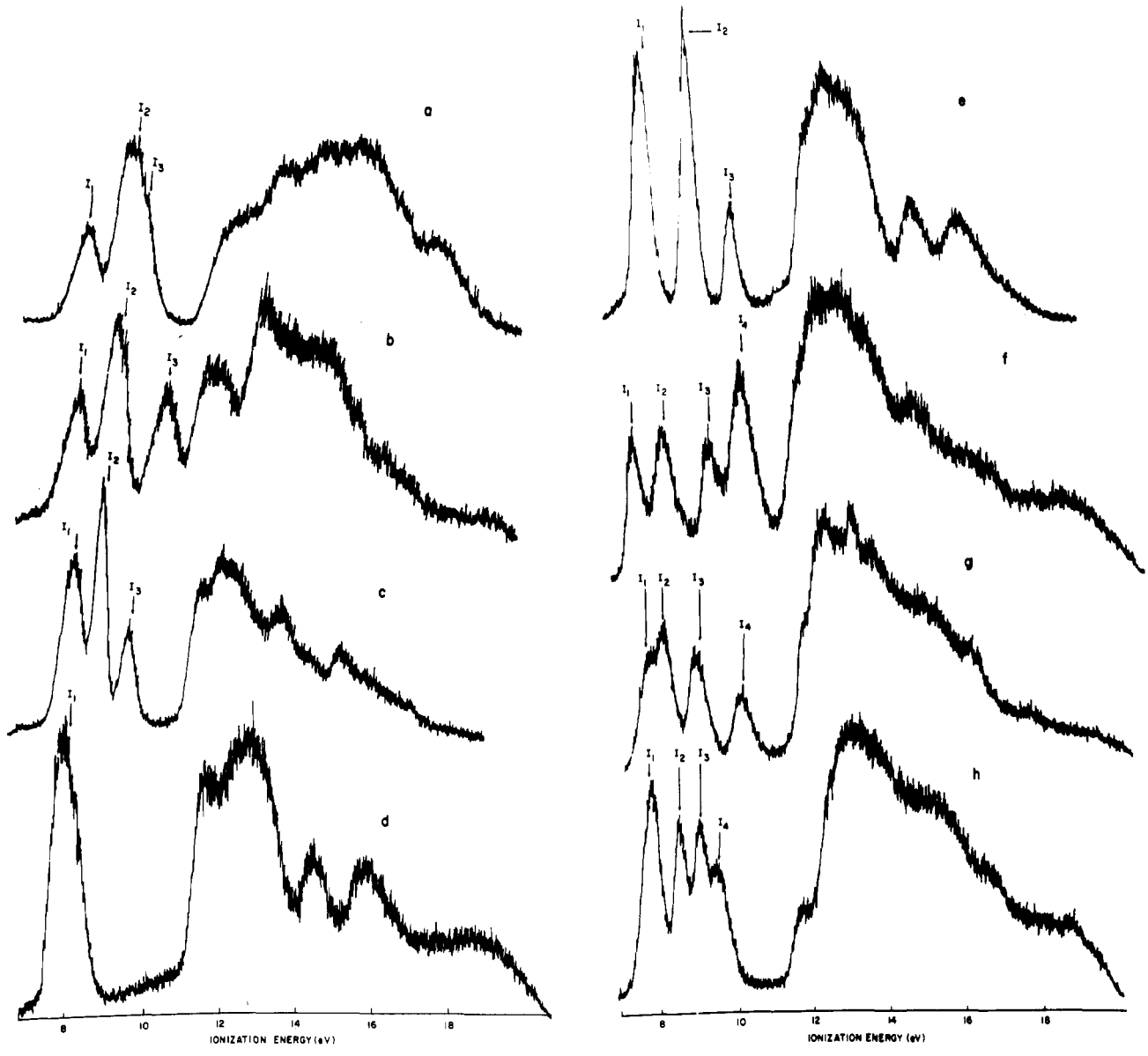

Figure 1. He I ultraviolet photoelectron spectra: (a) $P(NMeCH_2)_3CMe$ (**1**); (b) $OP(NMeCH_2)_3CMe$ (**1A**); (c) $SP(NCH_2CH_2)_3$ (**2B**); (d) $P(CH_2N)_3(CH_2)_3$ (**5**); (e) $SP(CH_2N)_3(CH_2)_3$ (**5B**); (f) $OP(CH_2N)_3(CH_2)_2(CH_2CH_2)$ (**6A**); (g) $P(NMe_2)_3$ (**7**); (h) $SeP(NMe_2)_3$ (**7C**).

portant structural features of **1A** and **1D** are (a) the PN_3 moiety is pyramidal and possesses C_{3v} symmetry, (b) the geometry at each nitrogen is trigonal planar, and hence the nitrogen lone pairs reside in essentially pure N 2p orbitals, and (c) the three N 2p lone-pair orbitals are coplanar, and each of them is orthogonal to the phosphorus lone-pair orbital. Given the rigid nature of these polycyclic systems, it seems safe to assume the persistence of the foregoing structural features throughout the series **1–1D**.

In the requisite C_{3v} symmetry the nitrogen lone-pair MO's, n_N, transform as $a_2 + e$, while the orthogonal phosphorus lone-pair MO, n_P, transforms as a_1. The sequence of MO stability $e > a_2$ follows from nodal-rule considerations.[3] The principal difficulty that arises when assembling a qualitative MO scheme for N–P compounds concerns the relative energies of the nitrogen and phosphorus lone-pair MO's prior to interaction. In isolated pyramidal MX_3 molecules (M = N, P, As, etc.) the IE's associated with electron ejection from the M lone-pair MO have been found[5] to be sensitive to, inter alia, (a) the electronegativity of M and (b) the X–M–X bond angle and hence the percent *n*s character in the M lone pair. Interestingly, the lone pair of IE's of Me_3N (8.54 eV)[5,6] and Me_3P (8.60 eV)[5,6,7] are almost identical. This near coincidence arises because the decrease of electronegativity in proceeding from N to P is approximately counterbalanced by the fact that the C–N–C bond angle in Me_3N (109°)[8] is larger than the C–P–C bond angle in Me_3P (100°);[8] i.e., the phosphorus lone-pair MO features more *n*s character.

As noted above, the nitrogen lone pairs of **1** reside in essentially pure 2p orbitals—a factor that should result in destabilization of the mean n_N in **1** compared to that in, e.g., Me_3N. This is one of the reasons that n_P is indicated to be more stable than n_N in Scheme Ia. There is also a more subtle effect at work. In a $P(NR_2)_3$ molecule with planar nitrogen geometries the P–N σ bonds feature ~33% N 2s character, while the same compound with tetrahedral nitrogens features ~25% N 2s character in the N–S bonding orbitals. Providing

(4) Clardy, J. C.; Kolpa, R. L.; Verkade, J. G. *Phosphorus Relat. Group V Elem.* **1974**, *4*, 133.
(5) Elbel, S.; Bergmann, H.; Ensslin, W. *J. Chem. Soc., Faraday Trans. 2* **1974**, *70*, 555.
(6) Cradock, S.; Ebsworth, E. A. V.; Savage, W. J.; Whiteford, R. A. *J. Chem. Soc., Faraday Trans. 2* **1972**, *68*, 934.
(7) Bock, H. *Pure Appl. Chem.* **1975**, *44*, 343.
(8) Sutton, L. E. *Spec. Publ.—Chem. Soc.* **1958**, *No. 11*.

Scheme I

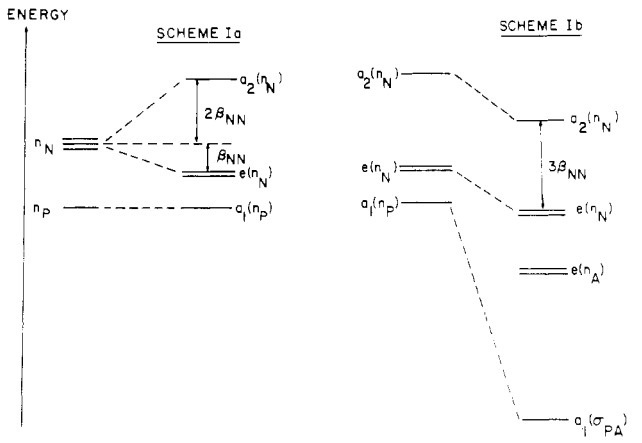

Scheme II

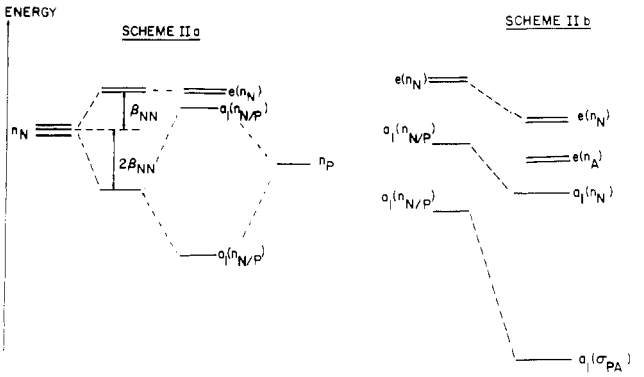

the N–P–N bond angles do not change, the aminophosphine with planar R_2N groups should have a more stable n_P orbital due to the increased effective group electronegativity.[9]

The UV PES of **1** (Figure 1a) is in conformity with Scheme Ia. Thus, peaks I_1 and I_2 correspond to the Koopmans states $^2A_2$ (n_N) and ^2E (n_N), respectively, while the $^2A_1$ (n_P) state appears as a shoulder (I_3) at 9.03 eV, on the second ionization. Note that the production of the ^2E state is accompanied by a Jahn–Teller splitting of ~0.17 eV.[10]

Several changes in the higher lying MO's are expected to take place when **1** coordinates to an acceptor, A. First, the n_P MO should stabilize appreciably as it becomes the P→A dative bond, σ_{PA} (Scheme Ib). Second, the $a_2(n_N)$ and $e(n_N)$ MO's are expected to stabilize somewhat due to the drift of charge from P to A. Finally, the $e(n_A)$ MO of the acceptor (chalcogen or BH_3 unit) is introduced.

Previous work has established that these ^2E states are produced in the following IE ranges: O ~10.0–11.5,[11,12] S ~8.5–11.0,[11,12] Se ~8.6–9.2,[12] and BH_3 ~10–12 eV.[13] Scheme Ib has been drawn on the assumption that the $e(n_A)$ MO is more stable than the $e(n_N)$ MO; i.e., A = O or BH_3. The order of these MO's would be reversed for A = S or Se. The use of Scheme Ib allows ready interpretation of the UV PES of **1A–1D**. For instance, in the UV PES of **1A** (Figure 1b), the relative intensities of peaks I_1 and I_2 suggest that they correspond to the generation of $^2A_2$ (n_N) and ^2E (n_N) Koopmans states, respectively. Like **1**, **1A** (and **1B–1D**) exhibit slight Jahn–Teller splitting of the ^2E (n_N) state (Table I). Peak I_3 in the UV PES of **1A**, clearly absent in the spectrum of the free ligand, **1**, is attributed to the production of the ^2E (n_O) state of the oxygen ligand. One further significant difference between the spectra of **1** and **1A** is the absence of a high-energy shoulder on peak I_2 of the latter. The work of Elbel and tom Dieck[11,12] has demonstrated that, typically, the n_P MO of a phosphine is stabilized by 2–3 eV upon phosphorus–oxygen bond formation. It can thus be surmised that the σ_{PO} ionization of **1A** is one component of the broad band between ~11.5 and 12.0 eV.

The UV PES of **1B–1D** (Table I) have been assigned by using a procedure similar to the one employed for **1A**. In the case of **1C**, the peak corresponding to electron ejection from the $e(n_{Se})$ MO completely masks that from the $a_2(n_N)$ MO.

The most noteworthy feature of the data that are summarized in Table I is the fact that the ionization energies of the nitrogen lone-pair MO's are remarkably constant in the complexes **1A–1D**. This is true, not only for the average nitrogen lone-pair energies, $\overline{IE_N}$,[14] but also for β_{NN}, the parameter that, within the structures of Koopmans' theorem,[15] measures the σ-type interaction between the a_2 and e nitrogen lone-pair MO's.[16] Since the a_2 MO of complexes **1A–1D** possesses unique symmetry (Scheme Ib), the energies of the $^2A_2$ (n_N) Koopmans state should respond only to inductive changes and thus fall in the order oxide > sulfide > selenide > borane. The observation that the energies of this state remain constant within experimental error suggests that the electron densities at phosphorus are very similar in these four compounds. One mechanism for achieving this is retrobonding from the acceptor to the phosphorus atom. Such $p_\pi(A)\rightarrow d_\pi(P)$ bonding is expected to be strongest when A = oxygen. Interestingly, a similar explanation has been advanced to explain trends in dipole moment[17] and NMR[18] data of phosphine oxides compared to those of other phosphine chalcogenides.

Turning now to compound series **2**, a recent X-ray structure determination of **2B**[19] has established that the nitrogen atoms are pyramidal (average ∠CNC = 109°) and that the nitrogen lone-pair axes are almost coplanar with the P–S bond and approximately 50° to this link. The same basic structure is assumed for the other members of the series. Like series **1**, series **2** features approximately C_{3v} skeletal geometry. However, the orientations of the nitrogen lone pairs differ by about 90° in the two series. For uncoordinated **2**, the phosphorus lone pair transforms as a_1 and the nitrogen lone pairs transform as $a_1 + e$. As shown in Scheme IIa, the $a_1(n_N)$ and $a_1(n_P)$ MO's are expected to be close in energy; hence a substantial interaction between them is expected. Unfortunately, however,

(9) For a discussion of group electronegativity, see: (a) Huheey, J. *J. Phys. Chem.* **1965**, *69*, 3284. (b) Hinze, J.; Jaffe, H. H. *J. Am. Chem. Soc.* **1962**, *84*, 540.

(10) The magnitudes of Jahn–Teller splittings vary appreciably and depend ultimately on the magnitudes of the quasielastic restoring forces. [For further discussion on this point, see: Rabalais, J. W. "Principles of Ultraviolet Photoelectron Spectroscopy"; Wiley-Interscience: New York, 1977; Chapter 9.] For N–P compounds, Jahn–Teller splittings are typically in the range 0.1–0.3 eV.[2a,e,f]

(11) Elbel, S.; tom Dieck, H. *J. Chem. Soc., Dalton Trans.* **1976**, 1757.

(12) Elbel, S.; tom Dieck, H. *J. Chem. Soc., Dalton Trans.* **1976**, 1762.

(13) (a) Lloyd, D. R.; Lynaugh, N. *J. Chem. Soc., Faraday Trans. 2* **1972**, *68*, 947. (b) Cowley, A. H.; Kemp, R. A.; Lattman, M.; McKee, M. *Inorg. Chem.*, in press.

(14) $\overline{IE_N}$ is the weighted (by orbital degeneracy) average of the n_N e and a_2 MO IE's.

(15) Koopmans, T. *Physica (Amsterdam)* **1934**, *1*, 104. There is no reason to suspect that Koopmans' theorem is violated for main-group systems such as the ones described here. Difficulties can arise, however, with electron ejection from transition-metal-localized MO's of certain organometallic compounds. See, for example: Cowley, A. H. *Prog. Inorg. Chem.* **1979**, *26*, 45.

(16) β_{NN} is calculated by taking the difference in IE of the n_N e orbitals (or average of the two maxima if Jahn–Teller split) and n_N a_2 orbital and dividing by 3. This may not be an accurate measure of the nitrogen lone-pair interaction if $p_\pi(N)\rightarrow d_\pi(P)$ bonding is appreciable. For T_d symmetry, as in **3**, δ_{NN} is the difference in IE between the t_2 and a_1 IE's divided by 4.

(17) Carlson, R. R.; Meek, D. W. *Inorg. Chem.* **1974**, *13*, 1741.

(18) Grim, S. O.; Walton, E. D. *Inorg. Chem.* **1980**, *19*, 1982.

(19) White, D. W.; Karcher, B. A.; Jacobson, R. A.; Verkade, J. G. *J. Am. Chem. Soc.* **1979**, *101*, 4921.

the free ligand **2** is not sufficiently stable to permit acquisition of UV PES data.[19] Furthermore, the low-IE peaks of the UV PES of the oxide (**2A**) and selenide (**2C**) are overlapped. Attention is therefore paid to interpretation of the UV PES of the sulfide (**2B**). In terms of an orbital synthesis (Scheme IIb) complexation of **2** to a sulfur atom will stabilize both a_1 MO's and the $e(n_N)$ MO. Of the two singly degenerate MO's, the lower a_1 ($n_{N/P}$) MO will be stabilized significantly on account of P→S bond formation; the higher a_1 MO will become somewhat more stable because of reduced interaction with the lower lying a_1 MO and also because of the charge redistribution that accompanies complexation. As in the case of Scheme Ib, it is necessary to introduce the acceptor lone-pair MO $e(n_A)$ into Scheme IIb. The UV PES of **2B** (Figure 1c) is in reasonable accord with the latter scheme. Thus, peaks I_1 and I_3 are ascribable to the production of the ^2E (n_N) and $^2A_1$ (n_N) Koopmans states, while the sharper, more intense peak, I_2, is due to electron ejection from the sulfur lone-pair MO, $e(n_S)$.[20] The σ_{PS} ionization appears at 11.8 eV. The UV PES of **2A** and **2C** can be interpreted in a similar manner to that of **2B**; however, as noted above, the spectra feature overlapping of peaks in the low-IE region.

One interesting feature that emerges from comparing the UV PES data of series **1** and **2** is the fact that β_{NN} for **2B** is ~60% larger than for any compound in the first series. The increase of β_{NN} is not due to structural differences since the N···N nonbonded distances are rather similar in **1A** (2.49 Å),[4] **1D** (2.60 Å),[4] and **2B** (2.59 Å).[19] Another interesting contrast between the two series is that qualitatively the nitrogen lone-pair ionizations in series **2** respond to the electronegativities of the acceptors. The reasons for the foregoing differences are not obvious, and detailed MO calculations on model compounds may be necessary.

Attention is now turned to the adamantane-like molecules **3**, **4**, and **5**–**5C**. The UV PES of urotropine (**3**) has, in fact, been published previously.[21] The present results are consistent with the literature data. Specifically, in the requisite T_d local symmetry the n_N MO's transform as $a_1 + t_2$ and, as usual, the energies of the Koopmans states are such that the $^2T_2$ state is produced at lower IE than the $^2A_1$ state. In fact, in the case of **3** the peak corresponding to production of the $^2A_1$ state is obscured by the σ-bonding "envelope". Replacement of one of the nitrogen atoms in **3** by a CMe group reduces the local symmetry of the three remaining nitrogen atoms in **4** to C_{3v}. Such an arrangement is similar to that in **2**; hence Scheme IIa (sans n_P interaction, of course) may be used for spectral interpretation. Thus, in the UV PES of **4** the first two peaks are assigned to the production of ^2E (n_N) and $^2A_1$ (n_N) Koopmans states as indicated in Table I. Replacement of one of the nitrogen atoms in **3** by a phosphorus atom results in **5**. As in **4** the nitrogen atoms in **5** reside in a C_{3v} environment, and hence the nitrogen lone pairs transform as $a_1 + e$. Introduction of the phosphorus lone pair results in an MO diagram like that at the right-hand side of Scheme IIa. However, in the UV PES of **5** (Figure 1d), note that there is only one low-energy peak (I_1). This observation suggests that the N/P interaction is sufficiently large that electron ejections from the $e(n_N)$ and $a_1(n_{N/P})$ MO's occur at almost identical ionization energies.[23] A further consequence of the large N/P interaction is that ionization of the lower lying $a_1(n_{N/P})$ MO occurs under the σ-bonding envelope. A lower limit of 11.8 eV for this ionization is therefore indicated in Table I. It is interesting to compare the UV PES of **3** and **5**. Since the IE's of nitrogen and phosphorus lone pairs are of similar magnitude, replacement of nitrogen by phosphorus is not expected to result in pronounced spectral changes. In this vein the first peak in the UV PES of **5** can be thought of as due to the production of a "quasi $^2T_2$" state.

Scheme III

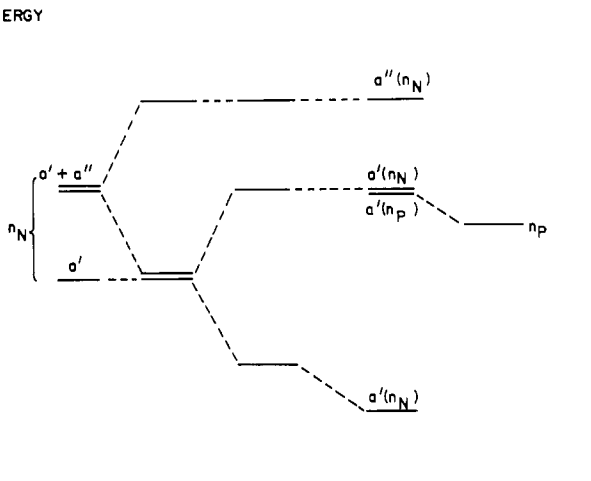

Coordination of the phosphorus lone pair of **5**[22] will produce orbital shifts very similar to those described for compound series **2** (Scheme IIb). Thus, in the UV PES of the sulfide, **5B** (Figure 1e), peaks I_1 and I_3 correspond to the production of the ^2E (n_N) and $^2A_1$ (n_N) Koopmans states while the sharper peak, I_2, is assigned to electron ejection from the sulfur lone-pair MO, $e(n_S)$. The UV PES of **5A** and **5B** can be assigned in a similar manner. Note that the trends in the IE's pertaining to the $e(n_N)$ and $e(n_A)$ MO's are very similar for **5A**–**5C** and **2A**–**2C**.

In compounds **6** and **6A** the molecular symmetry is lowered to C_s; hence the n_N orbitals transform as 2 a' + a'' and the n_P (or σ_{PO}) orbital possesses a' symmetry. The additional methylene group should raise the energy levels of the two similar nitrogen pairs in relation to the unique one. As shown in Scheme III, the two n_N MO's of a' symmetry interact to repel each other; additional interactions are caused by introduction of the phosphorus lone-pair MO, n_P. Note that the shift in the a'' (n_N) MO as **6** is coordinated to oxygen (0.28 eV) is less than the change in $\overline{IE_N}$ when **1** coordinates to oxygen. This trend is expected because of the intervening CH_2 groups in **6**. The peak at 10.5 eV in the UV PES of **6A** (Figure 1f) is assigned to electron ejection from the oxygen lone-pair MO's, a'(n_O) and a''(n_O). The absence of splitting in this ionization has been noted previously for other phosphine oxides of C_s symmetry.[12]

Acyclic Systems. The lack of rigidity of acyclic aminophosphines renders several conformations close in energy. This is one of the factors responsible for the controversy that has surrounded the interpretation of the UV PES of these compounds. In 1969 Vilkov and co-workers[24] investigated the structure of $(Me_2N)_3P$ (**7**) by gas-phase electron diffraction and concluded that this molecule possesses the propeller-type conformation, **A**.[25] In 1973 we investigated the UV PES of

(20) Electron removal from sulfur lone-pair MO's leads to characteristically sharp, intense UV PES peaks. See, for example ref 5 and 11 and: Cradock, S.; Whiteford, R. A. *J. Chem. Soc., Faraday Trans. 2* **1972**, *68*, 281.

(21) (a) Nelson, S. F.; Buschek, J. M. *J. Am. Chem. Soc.* **1974**, *96*, 7930. (b) Schmidt, W. *Tetrahedron* **1973**, *29*, 2129. (c) Dewar, M. J. S.; Worley, S. D. *J. Chem. Phys.* **1969**, *50*, 654.

(22) For the X-ray crystal structures of **5**, **5A**, and **5B**, see: Jogun, K. H.; Stezowski, J. J.; Fluck, E.; Weidlein, J. *Phosphorus Sulfur* **1978**, *4*, 199.

(23) In principle, the observation of only one low-IE peak could be ascribed to the absence of an N/P interaction. However, we prefer the interpretation presented in the text because all other compounds that we have studied exhibit appreciable N/P interactions.

(24) Vilkov, L. V.; Khaikin, L. S.; Evdokimov, V. V. *Zh. Strukt. Khim.* **1969**, *10*, 1101.

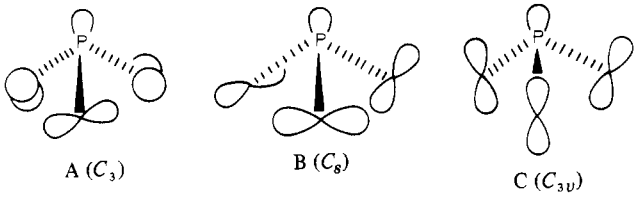

this molecule and suggested that the preferred conformation is B.[2a] The UV PES of **7** and cognates have subsequently been studied by others. Hargis and Worley[2h] and Yarbrough and Hall[2j] in essence agreed with our postulate, while Lappert et al.[2d] raised the possibility that tris(dialkylamino)phosphines adopt the C_{3v} conformation, C. Ab initio calculations[26] on the model compound, $(H_2N)_3P$, indicate that the C_3 conformation, A, represents a global minimum. However, the C_s conformation, B, is rather close in energy and could therefore be populated significantly at ambient temperature. X-ray structural results on more complex compounds also imply that conformations A and B are close in energy. Thus, in $(Me_2N)_3PFe(CO)_4$ the $(Me_2N)_3P$ ligand adopts an approximately C_3 geometry in which two of the Me_2N groups are nearly trigonal planar and twisted in the same direction, while the third Me_2N group is more pyramidal.[27] One of the $(Me_2N)_3P$ ligands of $[(Me_2N)_3P]_2Fe(CO)_3$ has a conformation virtually identical with that of $(Me_2N)_3PFe(CO)_4$; the other possesses approximately C_s skeletal symmetry.[26] Rømming and Songstad[28] have reported the X-ray crystal structures of $(Me_2N)_3PSe$, $(morpholino)_3P$, $(morpholino)_3PSe$, $(piperidino)_3P$, and $(piperidino)_3PSe$ and found that in each case the N_3P skeletal geometry corresponds roughly to either the C_3 (A) or C_s (B) conformation. More recently, Norman et al.[29] have reported that $(PhNH)_3P$ adopts the propeller-like conformation, A. Clearly, it would be desirable to determine the X-ray crystal structure of **7**. Unfortunately, however, X-ray diffraction experiments were precluded by the fact that **7**, a liquid at ambient temperature, freezes to a glass at lower temperatures.

Not only is the structure of **7** not certain but there are also uncertainties regarding the energies of the nitrogen and phosphorus lone-pair MO's. Scheme IVa should be regarded as somewhat heuristic in view of the foregoing discussion. One of the noteworthy features of Scheme IVa is that the initial energies of the nitrogen lone-pair MO's are differentiated. Thus, nitrogen lone pair 3, which is cis to the phosphorus lone pair, has more N 2s character than lone pairs 1 and 2, which are orthogonal to the phosphorus lone pair. Nitrogen lone pair 3, which transforms as a′ in C_s symmetry, therefore appears at lower energy than lone pairs 1 and 2. There should be little interaction between the two n_N MO's of a′ symmetry on account of their mutual orthogonality. Introduction of the phosphorus lone-pair MO, which transforms as a′, results in a strong conjugative interaction with nitrogen lone pair 3. Interpretation of the UV PES of **7** (Figure 1g and Table I) according to Scheme IVa implies that peaks I_1 and I_4 are associated with electron ejection from MO's of mixed nitrogen/phosphorus lone-pair character, while I_2 and I_3 correspond to ionization from predominantly nitrogen lone-pair character. Such a conclusion is in accord with Gaussian 76 and Xα calculations[2i] on the model compound $(H_2N)_3P$ in the C_s conformation.

Scheme IV

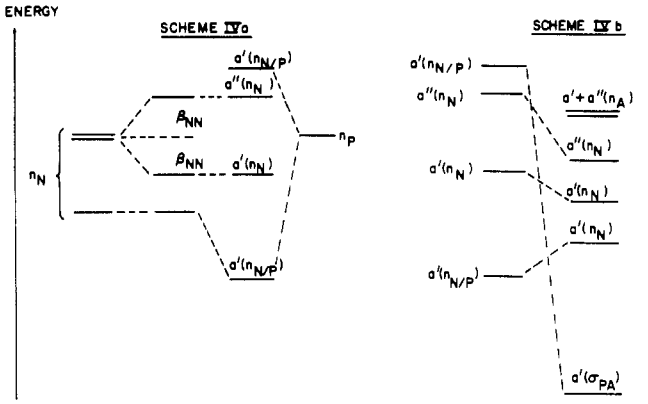

The selenide, $(Me_2N)_3PSe$ (**7C**), has been investigated by single-crystal X-ray diffraction[28b] and found to possess a skeletal structure close to C_s. The same structure has been assumed for **7A**, **7B**, and **7D**. As indicated in Scheme IIb, complexation of **7** to an acceptor should result in considerable stabilization of the HOMO, $a'(n_N/n_P)$, as it is converted into the P→A σ-bonding MO, $a'(\sigma_{PA})$. The other $a'(n_N/n_P)$ MO is expected to be destabilized in this process due to interaction with the newly formed σ_{PA} MO. Scheme IVb is completed by introduction of the a′ and a″ MO's of the acceptor. With the UV PES of $(Me_2N)_3PSe$ as an example (Figure 1h), the first peak is assigned to electron ejection from the n_{Se} orbitals of a′ and a″ symmetries. This assignment is supported by the large relative intensity of I_1. As pointed out above, the $^2A'$ and $^2A''$ states of acceptors are usually isoenergetic even in low-symmetry environments.[12] The assignments of the next three ionizations follow from Scheme IVb and are presented in Table I. The assignments for the UV PES of **7A**, **7B**, and **7D** (Table I) have been made in an analogous fashion. Finally, note that β_{NN} for **7D** is considerably less than the β_{NN} for **7A**–**7C**. The reason for this diminution in the nitrogen lone-pair interaction parameter is not immediately clear. It is possible that the nitrogen lone pairs are arranged differently in **7D**. The only known structure for this class of compound is that of $(H_2N)_3PBH_3$.[30] Unfortunately, however, the hydrogen atom positions were not well determined.

Experimental Section

Materials. Compounds **1**,[31] **1A**,[32] **1B**,[33] **1C**,[31] **1D**,[32] **2A**,[19] **2B**,[33] **2C**,[33] **3**,[34] **5**,[35] **5A**,[35] **5B**,[36] **6**,[37] **6A**,[37] **7**,[38] **7A**,[39] **7B**,[40] **7C**,[28] and **7D**[40] were prepared and purified as described in the literature. The preparation of **5C** was carried out analogously to that of **1C**.

Spectroscopic Measurements. All UV PES data were recorded on a Perkin-Elmer Model PS-18 photoelectron spectrometer using a He I photon source (21.22 eV). When necessary, the heated inlet probe was used to obtain suitable sample vapor pressures. Each spectrum was calibrated with a mixture of xenon (12.130 eV) and argon (15.759

(25) The drawings below imply that each nitrogen atom is trigonal planar and that the nitrogen lone pair resides in a pure 2p orbital. This is, of course, an idealization since, as discussed later, the geometry at nitrogen is contingent upon the dihedral angle along the N–P bond.
(26) Cowley, A. H.; Davis, R. E.; Lattman, M.; McKee, M.; Remadna, K. *J. Am. Chem. Soc.* **1979**, *101*, 5090.
(27) Cowley, A. H.; Davis, R. E.; Remadna, K. *Inorg. Chem.* **1981**, *21*, 2146.
(28) (a) Rømming, C.; Songstad, J. *Acta Chem. Scand., Ser. A* **1978**, *A32*, 689. (b) Rømming, C.; Songstad, J. *Ibid.* **1979**, *A33*, 187.
(29) Tarassoli, A.; Haltiwanger, R. C.; Norman, A. D. *Inorg. Nucl. Chem. Lett.* **1980**, *16*, 27.
(30) Nordman, C. D. *Acta Crystallogr.* **1960**, *13*, 535.
(31) Kroshefsky, R. O.; Weiss, R.; Verkade, J. G. *Inorg. Chem.* **1979**, *18*, 469.
(32) Kroshefsky, R. D.; Verkade, J. G. *Phosphorus Sulfur* **1979**, *6*, 391.
(33) Laube, B. G.; Bertrand, R. D.; Casedy, G. A.; Compton, R. D.; Verkade, J. G. *Inorg. Chem.* **1967**, *6*, 173.
(34) Hofman, A. W. *Ber. Dtsch. Chem. Ges.* **1869**, *2*, 153.
(35) Daigle, D. J.; Pepperman, A. B., Jr.; Vail, S. L. *J. Heterocycl. Chem.* **1974**, *11*, 407.
(36) Daigle, D. J.; Pepperman, A. B., Jr. *J. Heterocycl. Chem.* **1975**, *12*, 579.
(37) Daigle, D. J.; Pepperman, A. B., Jr. *J. Chem. Eng. Data* **1975**, *20*, 446.
(38) Burg, A. B.; Slota, P. J. *J. Am. Chem. Soc.* **1958**, *80*, 1107.
(39) Cowley, A. H.; Pinnell, R. P. *J. Am. Chem. Soc.* **1965**, *87*, 4454 and references therein.
(40) Reetz, T.; Katlafsky, R. *J. Am. Chem. Soc.* **1960**, *82*, 5036.

eV), which was used as an internal standard. Resolution was maintained between 20 and 50 meV for the argon line. All ionization energies were read as the band maxima unless noted otherwise and are the average of at least three different runs. Ionization energy data are accurate to ca. ±0.02 eV.

Acknowledgment. The authors are grateful to the National Science Foundation and the Robert A. Welch Foundation for generous financial support. We also thank Mr. D. E. Schiff for experimental assistance.

Registry No. **1**, 14418-26-9; **1a**, 15199-21-0; **1b**, 15199-22-1; **1c**, 68378-99-4; **1d**, 15199-24-3; **2a**, 71771-37-4; **2b**, 71771-38-5; **2c**, 71771-39-6; **3**, 100-97-0; **5**, 53597-69-6; **5a**, 53597-70-9; **5b**, 56796-56-6; **5c**, 79568-42-6; **6**, 56971-16-5; **6a**, 56971-17-6; **7**, 1608-26-0; **7a**, 680-31-9; **7b**, 3732-82-9; **7c**, 7422-73-3; **7d**, 7319-05-3.

Contribution from the Department of Chemistry, Florida Atlantic University, Boca Raton, Florida 33431

Electrochemistry, Spectroelectrochemistry, and Electron Paramagnetic Resonance Spectroscopy of Aqueous Molybdenum(VI), -(V), -(IV), and -(III) Catechol Complexes. Stabilization of Reduced Monomers in Weakly Alkaline Solution

LYNN M. CHARNEY, HARRY O. FINKLEA, and FRANKLIN A. SCHULTZ*

Received January 13, 1981

Stable, monomeric Mo(V), -(IV), and -(III) catechol complexes are generated by electrochemical reduction of the *cis*-dioxomolybdenum(VI) monomer $MoO_2(cat)_2^{2-}$ in pH >9 aqueous buffers containing excess catechol. The four oxidation states are interconverted within a range of ~450 mV. We have characterized the Mo(VI)–Mo(III) oxidation states by bulk solution electrochemistry, EPR spectroscopy, and visible wavelength spectroelectrochemistry in Hg(Au)-minigrid, thin-layer electrode cells. Coordination reactions at aquo sites produced upon reduction of Mo oxo groups stabilize the reduced monomers and influence their subsequent redox chemistry. The Mo(V) monomer is identified as $MoO(Hcat)(cat)_2^{2-}$, which bears a monodentate, monoprotonated catechol ligand cis to the Mo=O group. This monomer exists in equilibrium with 10–20% di-μ-oxo molybdenum(V) dimer at pH >9 and 1–2 mM Mo. The Mo(IV) and -(III) complexes are formulated as tris(catecholato) complexes which constitute a reversible $Mo(cat)_3^{2-/3-}$ redox pair. The former species may in fact contain coordinated semiquinone as $Mo^{III}(SQ)(cat)_2^{2-}$. This material is formed by two-electron reduction of $MoO(Hcat)(cat)_2^{2-}$ to $Mo(H_2O)(Hcat)(cat)_2^{2-}$, closure of the third catechol chelate ring in the Mo(III) electrode product, and *oxidative* transfer of one electron. At more positive potentials, $Mo(cat)_3^{2-}$ is oxidized irreversibly to the Mo(V) and -(VI) oxo species. Aqueous molybdenum–catechol electrochemistry therefore consists of structurally distinct Mo(VI)/Mo(V), Mo(V)/Mo(III), and Mo(IV)/Mo(III) redox couples cyclically linked by irreversible coordination and redox reactions.

In a previous paper[1] we described the electrochemistry of the *cis*-dioxo molybdenum(VI)–catechol complex, $MoO_2(cat)_2^{2-}$, in pH 3.5–7 aqueous buffers. Under these conditions, $MoO_2(cat)_2^{2-}$ is reversibly reduced to Mo(V) and Mo(III) monomers, but these species are only transiently stable. The principal means of deactivation after reduction to the Mo(V) state is dimerization, which proceeds through aquo or hydroxo sites on the metal. Partial coordination of pyridine at an aquo site on Mo(V) slows the rate but does not block the ultimate process of dimer formation.

Production of reduced molybdenum monomers in aqueous media is of interest in the bioinorganic and coordination chemistry of this element.[2] We therefore sought conditions which would stabilize monomeric electrode products by investigating the electrochemistry of $MoO_2(cat)_2^{2-}$ in more alkaline (pH 7–10) solutions. At pH ≥9 stable Mo(V), -(IV), and -(III) monomers can be generated electrochemically from $MoO_2(cat)_2^{2-}$. The present paper describes our efforts in characterizing these species and the processes by which they are formed using techniques of cyclic voltammetry, controlled-potential coulometry, EPR spectroscopy, and visible-wavelength spectroelectrochemistry[3] at optically transparent thin-layer electrodes.

Experimental Section

For spectroelectrochemical experiments, an optically transparent thin-layer electrode (OTTLE) cell with an amalgamated gold (Hg–Au) minigrid working electrode was constructed from a Teflon block following the design of Anderson et al.[4] A quartz plate was sealed against a silicone O-ring on the Teflon block by means of a pressure plate and four bolts. Internal Teflon strips served as spacers to control cell thickness. The gold minigrid (2000 lines/in., Buckbee-Mears Co., St. Paul, MN) was contained completely within the volume defined by the O-ring to avoid possible leakage across an O-ring/minigrid seal. Electrical contact with the grid was made by passing a gold rod through the Teflon block and sealing it in place with a hollow screw and a small O-ring. The entire cell could be readily disassembled for replacement of the gold mesh. The authors will provide details of construction upon request.

The published procedure for amalgamating a gold minigrid was modified. The cell was charged with a solution containing saturated mercuric nitrate, 0.5 M KCl, and 0.1 M HCl. Calomel (Hg_2Cl_2) was first deposited galvanostatically with a constant current of 100 μA and then converted to Hg^0 with use of either potentiostatic reduction at −0.4 V vs. SCE or further galvanostatic reduction at 100 μA. This two-step procedure eliminated excessive bubble formation and occasional breaks in electrical contact around the counter electrode of the OTTLE, which occurred if direct potentiostatic reduction of Hg^{2+} at −0.7 V was attempted. Other details of the amalgamation procedure were as described by Meyer et al.[5]

Visible spectra were recorded at a scan rate of 8 nm s^{-1} with the OTTLE cell in a rapid-scan spectrometer (RSS-C, Harrick Scientific Corp., Ossining, NY). For greater stability in these visible measurements, the xenon arc source was replaced by a 75-W tungsten–halogen lamp, powered by a 12-V dc supply (Hewlett-Packard 62012E). The RSS was interfaced to a Nova 2 minicomputer, which provided capabilities for acquisition of spectra, base-line subtraction, data smoothing, and data plotting. The optical thickness (ca. 250 μm) and coulometric volume (ca. 30 μL) of the cell were determined

(1) Charney, L. M.; Schultz, F. A. *Inorg. Chem.* **1980**, *19*, 1527.
(2) Stiefel, E. I. *Progr. Inorg. Chem.* **1977**, *22*, 1.
(3) Kuwana, T.; Heineman, W. R. *Acc. Chem. Res.* **1976**, *9*, 241. Heineman, W. R. *Anal. Chem.* **1978**, *50*, 390A.
(4) Anderson, C. W.; Halsall, H. B.; Heineman, W. R. *Anal. Biochem.* **1979**, *93*, 366.
(5) Meyer, M. L.; DeAngelis, T. P.; Heineman, W. R. *Anal. Chem.* **1977**, *49*, 602.

0020-1669/82/1321-0549$01.25/0